

ACCEPTED MANUSCRIPT • [OPEN ACCESS](#)

Functional 3D Structure Analysis of Quasispecies Variants of Hepatitis B Virus Surface and Core Protein in Advanced Liver Disease and Chronic HBV Infection Patients in Indonesia: In Silico

To cite this article before publication: Mahulette. S.J.A. et al. (2024). Functional 3D Structure Analysis of Quasispecies Variants of Hepatitis B Virus Surface and Core Protein in Advanced Liver Disease and Chronic HBV Infection Patients in Indonesia: In Silico. Jurnal Biota. In press
<http://jurnal.radenfatah.ac.id/index.php/biota/article/view/21681>

Manuscript version: Accepted Manuscript

Accepted Manuscripts is 'the version of the article accepted for publication including all changes made as a result of the peer review process, and which may also include the addition to the article by Jurnal Biota of a header, an article ID, a cover sheet and/or an 'Accepted Manuscript' watermark, but excluding any other editing, typesetting or other changes made by Jurnal Biota and/or its licensors'.

This Accepted Manuscript is © 2024 The Author(s). Published by Universitas Islam Negeri Raden Fatah Palembang

As the Version of Record of this article is going to be / has been published on a gold open access basis under a CC BY SA 4.0 International License, this Accepted Manuscript is available for reuse under a CC BY SA 4.0 International License immediately.

Everyone is permitted to use all or part of the original content in this article, provided that they adhere to all the terms of the license <https://creativecommons.org/licenses/by-sa/4.0/>

Although reasonable endeavors have been taken to obtain all necessary permissions from third parties to include their copyrighted content within this article, their full citation and copyright line may not be present in this Accepted Manuscript version. Before using any content from this article, please refer to the Version of Record on Pandawa Institute once published for full citation and copyright details, as permissions may be required. All third-party content is fully copyright protected and is not published on a gold open access basis under a CC BY SA license, unless that is specifically stated in the figure caption in the Version of Record.

View the [article online](#) for updates and enhancements.

1 **Functional 3D Structure Analysis of Quasispecies Variants of Hepatitis B**
2 **Virus Surface and Core Protein in Advanced Liver Disease and Chronic**
3 **HBV Infection Patients in Indonesia: In Silico**

4
5 **Samuel Johanes Aldrian Mahulette¹, Adhisa Fathirisari Putri¹, Azki Afidati Putri**
6 **Anfa¹, Yoshihiko Yano², Jajar Setiawan³, Wahyu Aristyaning Putri^{1*}**

7 ¹Department of Tropical Biology, Faculty of Biology, Universitas Gadjah Mada, Yogyakarta,
8 Indonesia

9 ²Department of Gastroenterology, Kobe University Hospital, Kobe, Japan

10 ³Department of Physiology, Faculty of Medicine, Public Health and Nursing, Universitas
11 Gadjah Mada, Yogyakarta, Indonesia

12
13 *Email: wahyuaristyaningputri@ugm.ac.id

14
15 **Abstract**

16 Hepatitis B Virus (HBV) is an endemic virus and belongs to Hepadnaviridae family. This virus
17 can result in variations of quasispecies due to its high rate of mutation. A quasispecies variant
18 is a small population and develops as a result of mutation and can become a wild-type
19 population. This research aims to study and carry out 3D modeling on 12 in-house full sequence
20 HBV genome isolates from Indonesia and obtain predictive visualization data to become a
21 reference for further research leading to the production of anti-virals and natural treatments for
22 HBV. 12 in-house full HBV genome sequences obtained from previous research were used to
23 carry out 3D modeling and structural analysis of the surface protein, core protein, and
24 polymerase protein. Analysis was carried out in silico using programs available online.
25 Phylogenetic analysis was carried out using MEGA11, translation of nucleotides into protein
26 sequences using the ExPASy Translate portal, physiochemical analysis using ProtParam portal,
27 and functional domain testing using the MOTIF tool from GenomeNet. Then 3D modelling
28 using Phyre2 and SWISS-MODEL. The major mutation of the S protein occurs in L21S and
29 mutations in the C protein mainly occur in P79Q and S87G. The model for S Protein from
30 homology structure prediction is not reliable thus it still needs more templates from
31 experimental techniques. While C Protein structure prediction can provide information for
32 further research in alternative natural antiviral treatment.

33 **Keywords:** 3D model, endemic, genome, HBV, protein.

35 **Introduction**

36 Hepatitis B Virus (HBV) is a leading cause of liver damage and liver tissue cancer
37 growth. Over 300 million people worldwide suffer from Chronic Hepatitis B (CHB), resulting
38 in 4 million deaths each year (Guvener & Arikan, 2020; Pastor *et al.*, 2019; Putri *et al.*, 2019).
39 Asia is home to over 70% of total HBV cases globally, with estimates suggesting this
40 percentage (Nguyen *et al.*, 2020; Thedja *et al.*, 2011; Muljono, 2017). In a joint research effort
41 in 2016, conducted by The Polaris Observatory Collaborators (2018), meta-analysis and
42 modeling were used to estimate the prevalence of HBsAg in 120 countries. This research
43 revealed that Indonesia ranked fourth in HBsAg-positive infections.

44 Indonesia, a Southeast Asian country, experiences high HBV endemicity due to its
45 unique archipelagic geography (Muljono, 2017; Thedja *et al.*, 2011). This geographical
46 isolation limits the availability of comprehensive databases for analyzing HBV variants'
47 pathogenicity and clinical characteristics. Nevertheless, in many cases of advanced liver
48 disease (ALD) and chronic HBV infection (CHB) among Indonesian patients, new
49 subgenotypes and genotype variants have been discovered (Yano *et al.*, 2015). Additionally,
50 researchers have identified 12 whole genome sequences of HBV quasispecies in ALD and CHB
51 patients in Java, all belonging to the dominant B3 genotype in the Southeast Asian region,
52 particularly Indonesia (Putri *et al.*, 2019).

53 Patients infected with HBV will be identified through laboratory diagnosis, which
54 involves checking the patient's serological status using markers or a combination of several
55 antigen markers, such as HB surface antigen (HBsAg), HB core antigen (HBcAg), HBeAg,
56 and/or antibody markers like HB surface antibody (anti-HBs/HBsAb), HB core antibody (anti-
57 HBc), HB e antibody (anti-HBe), and anti-HBc IgM (Guvener & Arikan, 2020; Nguyen *et al.*,
58 2020). The severity of HBV infection can also be determined by conducting the HBsAg,
59 HBeAg/anti-HBe, and HBV DNA tests, followed by assessing blood parameters such as
60 aspartate aminotransferase (AST) and alanine transaminase (ALT). Additionally, transient
61 elastography (Fibroscan) or needle liver biopsy can be used as non-invasive and invasive
62 methods for detecting liver cirrhosis (Guvener & Arikan, 2020).

63 HBV infection can lead to fibrosis in hepatocyte cells, and in chronic conditions, it can
64 progress to liver cirrhosis (LC). In the long term, HBV infection can also increase the risk of
65 hepatocellular carcinoma (HCC) or liver cancer (Guvener & Arikan, 2020; Nguyen *et al.*, 2020;
66 Putri *et al.*, 2019; van Hemert *et al.*, 2007). Liver cirrhosis is a condition affecting liver tissue,
67 characterized by the accumulation of regenerative nodules surrounded by fibrous fibers,

68 resulting from chronic liver tissue damage. This condition is preceded by collagen or fibrosis
69 encapsulation of damaged tissue (Schuppan & Afdhal, 2008).

70 In previous research, quasispecies were observed in the S and X regions of the HBV
71 ORFs (Putri *et al.*, 2019). Quasispecies variants are created due to viral replication mutations,
72 leading to diverse virus populations. These quasispecies populations are categorized into minor
73 populations (1-5%), intermediate populations (5-20%), and major populations (>20%). When
74 a mutant variant constitutes more than 80% of the population, it is considered to have replaced
75 the wild-type strain (Putri *et al.*, 2019; Yamani *et al.*, 2015). HBV is a virus that has diverse
76 DNA. The HBV genome consists of the X gene (X), precore/core gene (preC/C), presurface
77 antigen/surface antigen gene (preS/S), and polymerase gene (P) that control the replication and
78 transcription (Kim *et al.*, 2016; Campos-Valdez *et al.*, 2021). The HBV-X protein (HBx), is
79 involved in the pathological process of HBV and plays a major role in HBV replication by
80 either promoting viral replication or changing host gene expression linked to HCC (Kim *et al.*,
81 2016). HBx mutations have been implicated in the pathophysiology of HBV and are essential
82 for the development of HCC (Kim *et al.*, 2016; Zhang *et al.*, 2016). The core promoter region
83 (preC/C) contributes to the pathogenicity, morphogenesis, and essential for replication of the
84 virus (Kumar, 2022). The S gene (preS/S) encodes a series of surface antigen polypeptides that
85 are embedded inside the viral envelope, whereas the P gene encodes the reverse transcriptase
86 of the virus (Kim *et al.*, 2016). S gene mutations have the potential to impact HBsAg secretion,
87 immunogenicity, and antigenicity, and complicate illness diagnosis (Liu *et al.*, 2024). Models
88 of protein structure can be examined in silico. Utilizing in silico analysis, it was possible to
89 deduce the function of proteins, identify potential binding sites and partners for those
90 interactions, create or enhance new enzymes or antibodies, and explain the effects of current
91 mutations (Kryshtafovych and Fidelis, 2009). SWISS-MODEL and Phyre2 can used for
92 protein modelling (Basyuni *et al.*, 2018). In this study, we used 12 in-house full genome
93 sequences of HBV, including HBV genotype B3, to compare predicted protein structures.
94 These sequences were obtained from Putri *et al.*, 2019, with eight samples originating from LC
95 and/or HCC patients and four from CHB patients. Researchers suspect that the tertiary structure
96 of the protein surface will exhibit significant differences. However, the differences from the
97 wild-type genotype B3 may need to be more pronounced in the core protein and polymerase
98 protein.

99

100 **Materials and methods**

101 *Material and Methods*

102 1. *Retrieving in-house sequences*

103 In the previous research, thirty hepatitis B surface antigen (HBsAg)-positive were
104 collected at the General Hospital of Surabaya and Hajj Hospital (Surabaya, Indonesia), but only
105 twelve samples were successfully analyzed for the full genome. Twelve in-house isolates of
106 genotype B3 were obtained from previous research (Putri *et al.*, 2019). In this study, HBV
107 genotype B3 isolates were also used as the wild type. HBV DNA isolation was carried out
108 using the Qiagen DNA blood prep kit. The complete HBV genome was isolated using multiple
109 primer sets. Purification was conducted using the gel purification method (Qin *et al.*, 2011).
110 Direct sequencing was performed at PT. Genetika Science. The HBV genotype B3 sequence
111 from GenBank (<https://www.ncbi.nlm.nih.gov>) and the sequences of the 12 HBV isolates were
112 used for phylogenetic analysis. This analysis utilized the Clustal W tool from GenomeNet
113 (<https://www.genome.jp/tools-bin/clustalw>). Subsequently, a phylogenetic tree was
114 constructed using Molecular Evolutionary Genetics Analysis (MEGA) Software version 11.0.8
115 (<https://www.megasoftware.net/>) with 1000 bootstrap reconstructions (Putri *et al.*, 2019).

116

117 2. *Protein modelling*

118 The wild-type isolates and 12 in-house isolates were translated using the ExPASy
119 (Expert Protein Analysis System) Website Portal provided by the Biozentrum at the University
120 of Basel, Switzerland (<https://www.expasy.org/>). This bioinformatics portal and its tools are
121 hosted on an online server managed by the Swiss Institute of Bioinformatics (SIB). The
122 translation was performed by selecting the 'translate portal' (<https://web.expasy.org/translate/>).

123 Following translation, the ProtParam portal was utilized to conduct a physicochemical
124 analysis of the proteins translated from the 12 in-house and single wild-type isolates. The
125 physicochemical analysis covered molecular weight, amino acid composition, instability index,
126 half-life, aliphatic index, theoretical pI, and extinction coefficient (Gasteiger *et al.*, 2005).
127 Subsequently, the protein sequences of the 12 in-house isolates and the wild-type isolate were
128 assessed for functional domains using the MOTIF tool from GenomeNet
129 (<https://www.genome.jp/tools/motif/>). MOTIF sequences consist of amino acid compositions
130 that may hold biological significance (Bateman *et al.*, 2004).

131 SWISS-MODEL server (<https://swissmodel.expasy.org/>), used for modeling and
132 viewing ANOLEA and QMEAN6 values. ANOLEA measures model packaging quality by
133 estimating the average empirical atomic force magnitude, while QMEAN6 provides a global
134 and local assessment of the Qualitative Model Energy Analysis (Biasini *et al.*, 2014).
135 Homology modeling and evaluation of 3D structural models were conducted for 12 in-house

136 isolates and wild-type isolates using the Phyre2 website server hosted by the Imperial College
 137 of London (<http://www.sbg.bio.ic.ac.uk/phyre2/html/page.cgi?id=index>). Target isolates were
 138 submitted to the Phyre2 server in intensive modeling mode, and the modeling process relied
 139 on data retrieved from the Protein Data Bank (PDB). Alignment scores were generated for the
 140 top 10 structures, which were then used to create 3D models. Model quality was assessed based
 141 on their similarity to the template model (Kelley *et al.*, 2015).

142

143 Results

144 1. Mutation mapping

145 Sequences of S and C proteins from eight samples from Putri *et al.* (2019) conducted
 146 using SWISS-MODEL software are shown in Table 1 and Table 2. Mutations in the S and C
 147 proteins occur sporadically but are more common in ALD than in CHB patients. The major
 148 mutation of the S protein occurs in L21S and mutations in the C protein mainly occur in P79Q
 149 and S87G (Table 1). The results of this study are slightly different from research by Huong *et*
 150 *al.* (2022), where the hot mutations in the S protein from HBV-CHB patients were S53L
 151 (37,7%), A184V/G (39,3%), and S210K/N/R/S (39,3%), while L21S was only around 29,1%.
 152 In other research from Wahyuni *et al.* (2019), mutations in ALD patients were more common
 153 in T1631C (65,6%), and no mutations in L21S, P79Q, and S87G.

154 **Table 1. Protein sequence alignment and mutation mapping of the S Protein. 12 In-**
 155 **house S Protein Query were align with HBV Genotype B3 (AB713527.1)**

Genotype B3	A	L	Q	N	G	L	Q	S	C
A1 ALD	T
B1 ALD	E
C1 ALD	S	S
D1 ALD	Y
A2 ALD	.	S	R	.	E
C2 ALD	T	S	.	S	.	.	.	N	.
D2 ALD
E2 ALD
F1 CHB	P	.	.
G1 CHB
B2 CHB	Y
F2 CHB	.	S	.	.	E	P	.	.	.

156

157 **Figure 2. Protein sequence alignment and mutation mapping of the C Protein. 12 In-house**
 158 **S Protein Query were align with HBV Genotype B3 (AB713527.1)**

Genotype B3	P	V	I	L	Y	S	I	S	E	P	E	S
A1 ALD	T	.	G	.	Q	.	.
B1 ALD	T	Q	D	G
C1 ALD	.	A	G
D1 ALD
A2 ALD	T	Q	D	G
C2 ALD	.	.	V	.	.	T	V	.	Q	.	.	N
D2 ALD
E2 ALD
F1 CHB	T	Q	.	G
G1 CHB
B2 CHB	Q	Q	.	.
F2 CHB	.	.	.	M	F	G

159

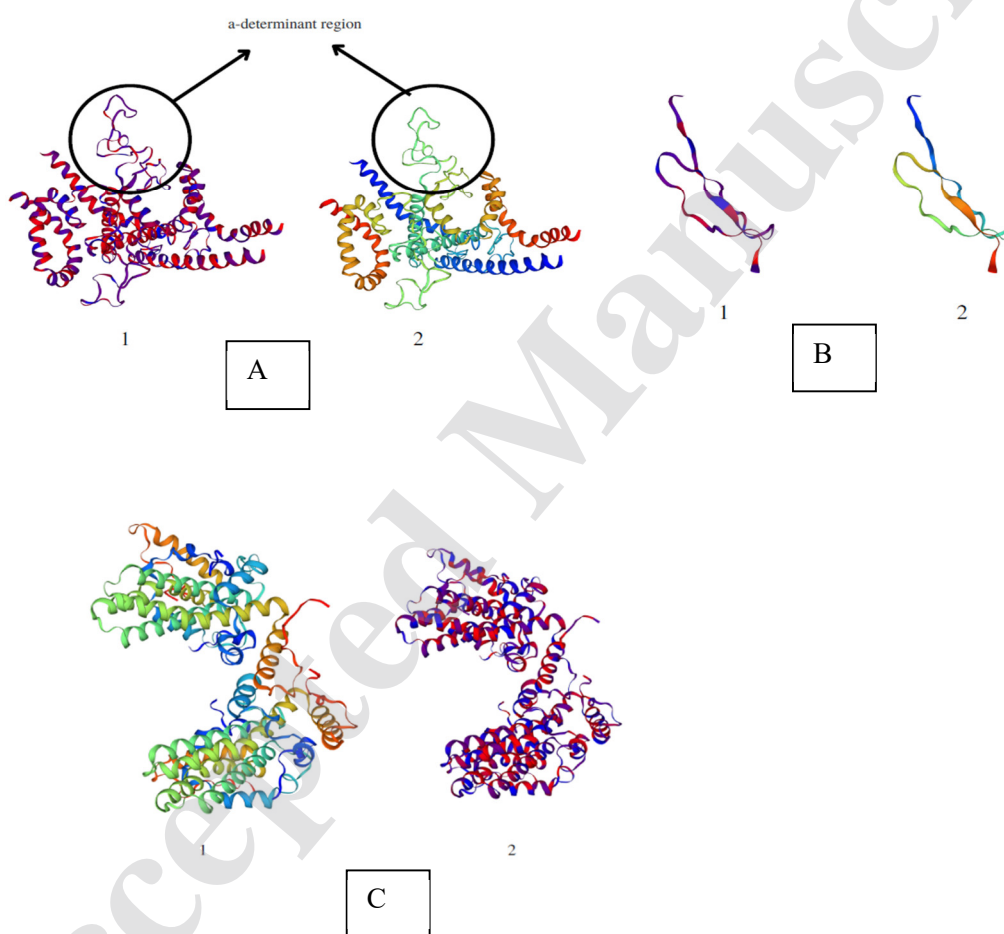
160 **2. Protein structure prediction SWISS-MODEL**

161 Protein structure prediction with SWISS-MODEL on the S protein produces two
 162 models, each containing two structures. Model 1 is built based on the Woodchuck Hepatitis
 163 Virus homodimer, and Model 2 is built based on the heterodimer Tumor necrosis factor
 164 receptor superfamily member five and only covers 33 aa (118-151) in the MHR and the a-
 165 determinant part of the S protein. Model C protein has a homo-tetramer oligo state. The outside
 166 of Model C protein consists of the least hydrophobic layer, with a hydrophobic layer inside
 167 (Figure 1). The Qmean Z-score results on the S and C protein structures with SWISS-MODEL
 168 are listed in Table 1. Qmean Z-Score -7.74 on Model 1 predicts a low-quality model (below -
 169 4.0). Qmean Z-Score -3.93 on Model 2 predicts a good quality model (above -4.0). Qmean Z-
 170 Score on C Protein predicts a good quality model (above -4.0).

171 **Table 3. Qmean Z-Score for protein structure from SWISS-MODEL**

Structure	Qmean Z-Score				
	Qmean	C β	All atom	Solvation	Torsion
S Protein (Model 1)	-7,74	-7,67	-2,97	-3,03	-5,63
S Protein (Model 2)	-3,93	-0,78	-1,24	-2,58	-3,68
C Protein	-1,06	-2,41	0,77	0,56	-0,87

172



173

174 **Figure 1.** S Protein structure prediction from SWISS-MODEL (A) Model 1 (B) Model 2.
 175 Structure (1) color annotation by the hydrophobicity of the protein; the red color on the
 176 annotation represents the most hydrophobic region. Blue color depicts the least hydrophobic
 177 region. Structure (2) color annotation rainbow respectively from N-terminus to C-terminus. C
 178 Protein structure prediction from SWISS-MODEL (C). Structure (1) color annotation by the
 179 hydrophobicity of the protein; red color on the annotation represents the most hydrophobic

180 region. Blue color depicts the least hydrophobic region. Structure (2) color annotation rainbow
181 respectively from N-terminus to C-terminus.

182

183 3. Protein structure prediction Phyre2

184 Protein structure prediction was done using Phyre2 software, as in Figure 2. S Protein
185 Structure from Phyre2 has a bad quality assessment. Most of the structures were modeled by
186 ab initio. S Protein modeled by Phyre2 does not have any pocket proteins. C Protein Structure
187 from Phyre2 has a good quality assessment (Figure 3). Most of the structures were modeled
188 from updated template. Based on conservation and pocket detection analysis, aa K96 to F110
189 are the most conserved regions with four protein pocket sites.

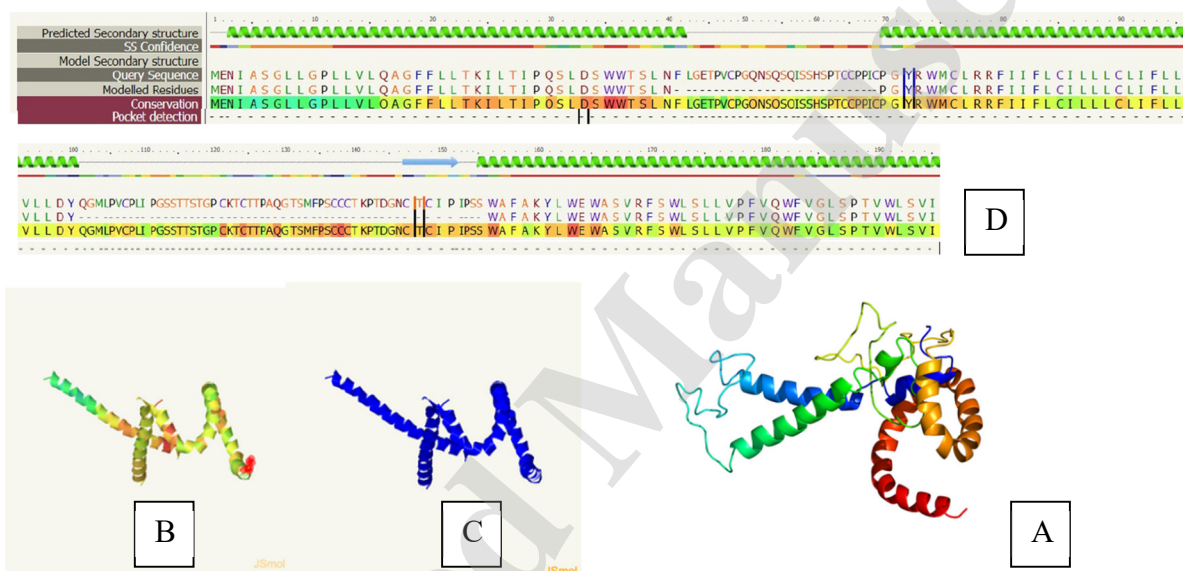


Figure 2. (A) S Protein structure prediction from Phyre2 (B) Conservation site analysis of the predicted model (C) Pocket detection site analysis of the predicted model. (D) Complete query of the S Protein predicted secondary structure along with the confidence level and analysis result of conservation and pocket detection analysis.

190

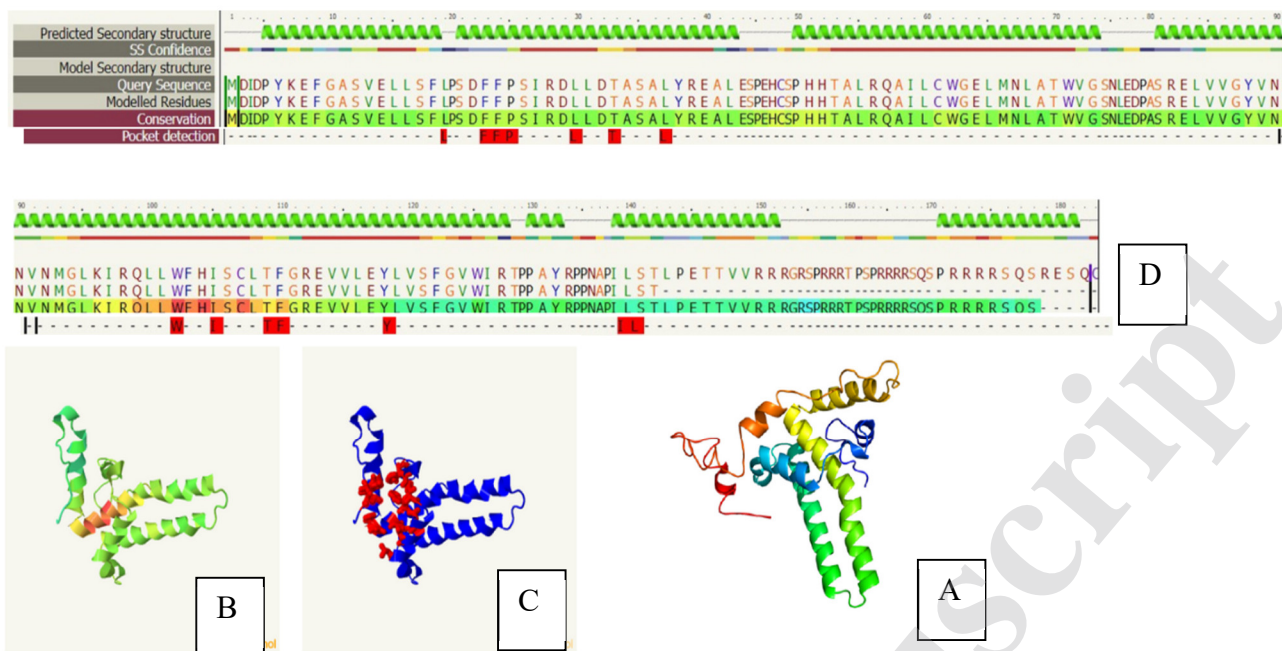


Figure 3. (A) C Protein structure prediction from Phyre2 (B) Conservation site analysis of the predicted model (C) Pocket detection site analysis of the predicted model. (D) Complete query of the C Protein predicted secondary structure along with the confidence level and analysis result of conservation and pocket detection analysis.

191 4. Protein ligand binding SWISS-MODEL

192 Protein-ligand binding analysis was carried out with SWISS-MODEL on S protein and
 193 C protein with a nonbonded interaction graph, as in Figure 4 There is a slight potential to block
 194 S Protein based on ligand hotspot analysis from Model 1. Hotspot aa W36 has the highest
 195 nonbonded interaction of 9.14% on Model 1 (Figure 4A). Model 2 has the highest nonbonded
 196 interaction of 22.13% on hotspot T125 (Figure 4B). Nonbonded interaction in Model 2
 197 potentially provides more information regarding ligand blocking of S Protein as an alternative
 198 treatment. The C protein hotspot aa W102 has the highest average nonbonded interaction of
 199 6.03% (Figure 4C). Followed by L37.B of 5.81%. Hotspot aa W102 is also a protein pocket
 200 site and the most conserved site based on SWISS-MODEL analysis. There is a potential to bind
 201 C Protein using alternative compounds.

202

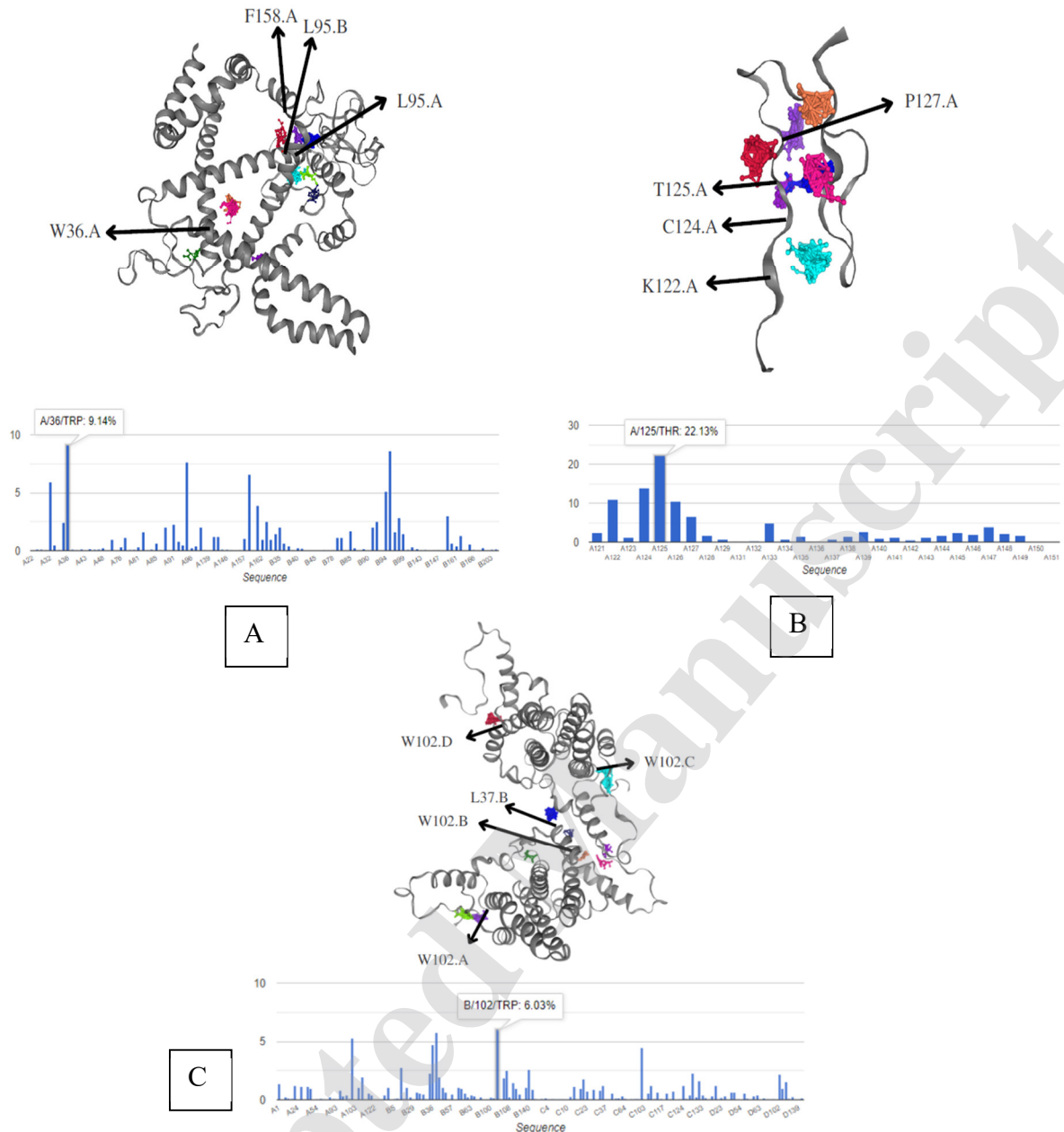


Figure 4. S Protein ligand binding analysis (A) Model 1 S Protein from SWISS-MODEL with nonbonded interaction graph (B) Model 2 S Protein from SWISS-MODEL with nonbonded interaction graph. (C) C Protein ligand binding analysis from C Protein modelled by SWISS-MODEL with nonbonded interaction graph.

203

204 Discussion

205 HBV currently consists of at least 9 genotypes (A to I), with 96% of chronic HBV
 206 infections generally caused by genotypes C (26%), D (22%), E (18%), A (17%), and B (14%)
 207 (Yano *et al.*, 2015; Velkov *et al.*, 2018). Generally, Indonesia is dominated by genotype B and
 208 subgenotype B3, unlike other Asian countries, which are dominated by subgenotypes B1 and

209 B2 (Gao *et al.*, 2019). The absence of in-silico research on the B3 subgenotype in Indonesia
210 limits the comparability of our findings with other studies.

211 Mutations in the B3 subgenotype were analyzed using SWISS-MODEL software. L21S
212 is the main mutation in the S protein (Table1), and P79Q and S87G are in the C protein (Table
213 2). Mutations in the S protein are associated with several liver disorders (Jiang *et al.*, 2021).
214 Another study showed that mutations in the HBV genotype may cause liver cirrhosis and could
215 act as molecular markers for the diagnosis of the clinical symptoms of chronic HBV disease
216 (Kumar, 2022; Chen *et al.*, 2005).

217 SWISS-MODEL and Phyre2 software are used to predict protein structures based on
218 current sequences. SWISS-MODEL provides quality estimates at several stages of the
219 modeling process to help the user identify optimal templates and is also utilized for the fully
220 automated template selection procedure. Once models have been built, their quality is assessed
221 by the QMEAN scoring function (Z-score) (Waterhouse *et al.*, 2018). S Protein has two
222 different models (model 1 and model 2), and only model 2 shows good quality (Figure 1, Table
223 3). Model 1 was analyzed with homodimer Woodchuck hepatitis virus (WHV) and had a Z-
224 score value of -7.14. The woodchuck model system is a vital instrument of natural viral
225 infection. HBV and WHV infections and virions are identical. Because the genomes of HBV
226 and WHV can resemble one other by up to 65%, comparing the two viruses is crucial for the
227 development of antivirals (Kukreja *et al.*, 2024). Model 2 was analyzed with heterodimer tumor
228 necrosis factor receptor and had a Z-score value of -3.93. This shows that model 2 is more
229 effective in developing antivirals compared to model 1. Tumor necrosis factor-alpha-induced
230 protein 1 (TNF- α IP1) was shown to be more highly expressed in HBV (Lin *et al.*, 2005). In
231 addition, tumor necrosis factor-alpha (TNF-alpha) can detect HBV infection and inhibit viral
232 DNA replication in mouse animal models (Tzeng *et al.*, 2014). The region highlighted as "a
233 determinant" in model 1 (Figure 1A) is part of the surface gene. It's prone to mutations that can
234 lead to various issues like immune evasion and vaccine resistance. Mutations in the S gene can
235 cause amino acid substitutions, particularly in the HBsAg "a determinant" area. These
236 substitutions can reduce sensitivity in diagnostic tests and lead to failures in response to both
237 the Hepatitis B vaccine (HepB) and Hepatitis B Immunoglobulin (HBIG). These mutations,
238 known as vaccine escape mutations, were reported by Ko *et al.* (2020). Hsu *et al.* (2010) found
239 a higher incidence of these mutations in children who received plasma-derived vaccines (0.3%)
240 compared to those who received recombinant vaccines (0.06%). The C protein has a homo-
241 tetramer oligo state with a Z-score value of -1,06. Mutations in the core protein are known to
242 cause severe liver disease disorders such as liver fibrosis, cirrhosis, and hepatocellular

243 carcinoma (Mohamadkhani *et al.*, 2009; Al-Qahtani *et al.*, 2018). In this study, the C protein
244 consists of the least hydrophobic layer. According to Pastor *et al.* (2019), the interaction of
245 mutants L60, L95, and K96 between L protein and C protein occurs in the hydrophobic area
246 preventing the development of mature viruses. Therefore, the C protein model can also be used
247 as a reference for the development of antiviral treatment.

248 Conservation and pocket detection are functional parameters in Phyre2 protein structure
249 analysis. The conservation model can provide information on the possibility of the presence or
250 absence of a functional residue. Color indicators ranging from green to red indicate residue
251 areas with high conservation value; the closer to red, the higher the conservation value (High).
252 Meanwhile, color indicators from green to purple have a low conservation value; the closer to
253 purple, the lower the conservation value (Low). Pocket detection is one of the functional
254 protein parameters used to predict which amino acids can be used as active sites. The largest
255 pocket is often found as an active site location. The largest pocket detected by the fpocket2
256 program (le Guilloux *et al.*, 2009) is shown in red wireframe mode. Pocket detection was not
257 detected in the S Protein (Figure 2C) but was detected in the C protein with four active pocket
258 sites (Figure 3C). The hydrophobic pocket of an external component can be bound by the HBV
259 capsid. According to Lecoq *et al.* (2021), the homolog of Triton X-100 is predicted to disrupt
260 the HBV life cycle by either engaging in competition with the natural pocket factor or by
261 impeding capsid dynamics into a single conformation. A novel target for medication to
262 intervene in the HBV life cycle is the hydrophobic pocket. This allows the C protein to bind to
263 the HBV capsid and inhibit the process of transferring genetic material and HBV replication.
264 The results suggest that the S Protein model requires additional templates to improve its quality,
265 while the C protein model exhibits better quality and can serve as a reference for future
266 research.

267 Research on the interactions between proteins and ligands is crucial to knowing the
268 mechanism of biological regulation. This technique can identify potentially active compounds
269 with the greatest for developing drugs and forecast the binding affinity of molecules inside
270 certain receptor targets (Fu *et al.*, 2018). In this study, hotspot aa W36 has the highest
271 nonbonded interaction of 9.14% on Model 1 of S protein (Figure 4A), whereas model 2 has
272 the highest nonbonded interaction of 22.13% on hotspot T125 (Figure 4B). The C protein
273 hotspot aa W102 has the highest average nonbonded interaction of 6.03% (Figure 4C),
274 followed by L37.B of 5.81%. Hotspots were often linked to protein areas that bind low
275 molecular weight molecules, a single ligand that has the same moiety as a substructure, and a
276 single binding subpocket across various structures (Wakefield *et al.*, 2020). Protein C shows a

277 lower affinity value between model 1 and model 2 of S protein. Lower values signify a stronger
278 hydrogen bond between the drug and the protein receptor as well as a greater binding affinity
279 (Uzzaman *et al.*, 2019; Thafar *et al.*, 2022). In addition, hotspot aa W102 of C protein is also a
280 protein pocket site and the most conserved site based on SWISS-MODEL analysis. There is a
281 potential to bind C Protein using alternative compounds.

282

283 **Conclusions**

284 Mutations in the B3 subgenotype consist of S protein mutations (L21S) and C protein mutations
285 (P79Q and S87G) which cause chronic HBV in Indonesia. The model for S Protein from
286 homology structure prediction can be said to be reliable thus it still needs more templates from
287 experimental techniques. While C Protein structure prediction can provide information for
288 further research in alternative natural antiviral treatment supported by a Z-score value above -
289 4.0, has four active pocket site, and has the highest binding affinity capability..

290

291 **References**

- 292 Al-Qahtani, A., Al-Anazi, M.R., Nazir, N., Abdo, A.A., Sanai, F.M., Al-Hamoudi, W.K.,
293 Alswat, K.A., Al-Ashgar, H.I., Khan, M.Q., Albenmoussa, A., El-Shamy, Alanazi, S.K.,
294 Cruz, D.D., Bohol, M.F., Al-Ahdal, M.N. (2018). The correlation between hepatitis B
295 virus precore/core mutations and the progression of severe liver disease. *Front Cell Infect*
296 *Microbiol*, 8:355. doi: 10.3389/fcimb.2018.00355
- 297 Ahang, Z.H., Wu, C.C., Chen, X.W., Li, X., Li, J., Lu, M.J. (2016). Genetic variation of of
298 hepatitis B virus and its significance for pathogenesis. *World J Gastroenterol*, 22(1):126-
299 44
- 300 Basyuni, M., Wati, R., Sulistiyono, N., Hayati, R., Sumardi, Oku, H., Baba, S., Sagami, H.
301 (2018). Protein modelling of triterpene synthase genes from mangrove plants using
302 Phyre2 and Swiss-model. *International Conference on Computing and Applied*
303 *Informatics* 2017, 978, 012095
- 304 Bateman, A., Coin, L., Durbin, R., Finn, R.D., Holich, V., Griffiths-Jones, S., Khanna, A.,
305 Marshall, M., Moxon, S., Sonnhammer, E.L.L., Studholme, D.J., Yeats, C., Eddy, S.R.
306 (2003). The Pfam protein families database. *Nucleic Acids Research*, 32: D138-D141. doi:
307 10.1093/nar/gkh121
- 308 Biasini, M., Bienert, S., Waterhouse, A., Arnold, K., Studer, G., Schmidt, T., Kiefer, F.,
309 Cassarino, T.G., Bertoni, M., Bordoli, L., Schwede, T. (2014). SWISS-MODEL:
310 modelling protein tertiary and quaternary structure using evolutionary information.

311 *Nucleic Acid Research*, 42: 1-7. doi: 10.1093/nar/gku340

312 Campos-Valdez, M., Monroy-Ramirez, H.C., Armendariz-Borunda, J., Sanchez-Orozco, L.V.
313 (2021). Molecular mechanisms during Hepatitis B infection and the effects of the virus
314 variability. *Viruses*, 13(6), 1167

315 Chen, C.H., Lee, C.M., Lu, S.N., Changchien, C.S., Eng, H.L., Huang, C.M., Wang,
316 J.H., Hung, C.H., Hu, T.H. (2005) Clinical significance of hepatitis B virus (HBV)
317 genotypes and precore and core promoter mutations affecting HBV e antigen expression
318 in Taiwan. *J Clin Microbiol.* 2005;43:6000-6006.

319 Fu, Y., Zhao, J., Chen, Z. (2018). Insights into the molecular mechanisms of protein-ligand
320 interactions by molecular docking and molecular dynamics simulation: A case of
321 oligopeptide binding protein. *Comput Math Methods Med*, 2018:3502514. doi:
322 10.1155/2018/3502514

323 Gasteiger, E., Hoogland, C., Gattiker, A., Duvaud, S., Wilkins, M.R., Appel, R.D., Bairoch, A.
324 (2005). *Protein Identification and Analysis Tools on the ExPASy Server*. Humana Press.
325 Totowa. pp. 571-607. doi: 10.1385/1-59259-890-0:571

326 Guvenir, M. and Arikan, A. (2020). Hepatitis B virus: from diagnosis to treatment. *Polish*
327 *Journal of Microbiology*, 69 (4): 391-399. <https://doi.org/10.33073/pjm-2020-044>

328 Hsu, H.Y., Chang, M.H., Ni, Y.H., Chiang, C.L., Chen, H.L., Wu, J.F., Chen, P.J. (2010). No
329 increase in prevalence of hepatitis B surface antigen mutant in a population of children
330 and adolescents who were fully covered by universal infant immunization. *JID* 2010:201.

331 Kelley, L.A., Mezulis, S., Yates, C.M., Wass, M.N., Sternberg, M.J.E. (2015). The Phyre2 web
332 portal for protein modeling, prediction and analysis. *Nature Protocols*, 10 (6): 845-858.
333 doi: 10.1038/nprot.2015.053

334 Kim, H, Lee, S.A., Kim,B.J. (2016). X region mutations of hepatitis B virus related to clinical
335 severity. *World J Gastroenterol*, 22(24): 5467-5478

336 Ko, K., Takahashi, K., Nagashima, S., Yamamoto, C., Ork, V., Sugiyama, A., Akita, T., Ohisa,
337 M., Chuon, C., Hossain, M.S., Mao, B., Tanaka, J. (2020). Existence of hepatitis B virus
338 surface protein mutations and other variants: demand for hepatitis B infection control in
339 Cambodia. *BMC Infectious Diseases* (2020) 20:305. [https://doi.org/10.1186/s12879-020-](https://doi.org/10.1186/s12879-020-05025-3)
340 [05025-3](https://doi.org/10.1186/s12879-020-05025-3)

341 Kryshtafovych A, Fidelis K. (2009). Protein structure prediction and model quality assessment.
342 *Drug Discov Today*, 14(7-8):386-93

343 Kukreja, A.A., Wang, J.C., Pierson, E., Keifer, D.Z., Selzer, L., Tan, Z., Dragnea, B., Jarrold,
344 M.F., Zlotnick, A. (2014). Structurally similar woodchuck and human hepadnavirus

345 core proteins have distinctly different temperature dependences of assembly. *J Virol*,
346 88(24): 14105-15. doi: 10.1128/JVI.01840-14Kumar, R. (2022). Review on hepatitis B
347 virus precore/core promoter mutations and their correlation with genotypes and liver
348 disease severity. *World J Hepatol*, 14(4): 708-718 DOI: 10.4254/wjh.v14.i4.708

349 le Guilloux, V., Schmidtke, P., Tuffery, P. (2009). Fpocket: An open source platform for
350 ligand pocket detection. *BMC Bioinformatics*, 10 (168). doi:10.1186/1471-2105-10-168.

351 Lecoq, L., Wang, S., Dujardin, M., Zimmermann, P., Schuster, L., Fogeron, M.L., Briday, M.,
352 Schledorn, M., Wiegand, T., Cole, L., Montserret, R., Bressanelli, S., Meier, B.H.,
353 Nassal, M., Bockmann, A. (2021). A pocket-factor-triggered conformational switch in
354 the hepatitis B virus capsid. *Proc Natl Acad Sci USA*, 118(17):e2022464118. doi:
355 10.1073/pnas.2022464118Lin, M.C., Lee, N.P., Zheng, N., Yang, P.H., Wong, O.G.,
356 Kung, H.F., Hui, C.K., Luk, J.M., Lau, G.K. (2005). Tumor necrosis factor-alpha-
357 induced protein 1 and immunity to hepatitis B virus. *World J Gastroenterol*,
358 11(48):7564-8. doi: 10.3748/wjg.v11.i48.7564

359 Liu, H., Chen, S., Liu, X., Lou, J. (2024). Effect of S-region mutations on HBsAg in HBsAg-
360 negative HBV-infected patients. *Virology Journal*, 21(92).

361 Muljono, D.H. (2017). Epidemiology of hepatitis B and C in Republic of Indonesia. *Euroasian*
362 *Journal of Hepato-Gastroenterology*, 7 (1): 55-59. doi: 10.5005/jp-journals-l0018-1212

363 Mohamadkhani, A., Jazii, F.R., Poustchi, H., Nouraein, O., Abbasi, S., Sotoudeh, M.,
364 Montazeri, G. (2009). The role of mutations in core protein of hepatitis B virus in liver
365 fibrosis. *Virol J*, 6: 209. <https://doi.org/10.1186/1743-422X-6-209>

366 Nguyen, M.H., Wong, G., Gane, E., Kao, J., Dusheiko, G. (2020). Hepatitis B virus: advances
367 in prevention, diagnosis, and therapy. *Clinical Microbiology Reviews*, 33 (2): 1-38.
368 <https://doi.org/10.1128/CMR.00046-19>

369 Pastor, F., Herrscher, C., Patient, R., Eymieux, S., Moreau, A., Burlaud-Gaillard, J., Seigneuret,
370 F., de Rocquigny, H., Roingeard, P., Hourieux, C. (2019). Direct interaction between the
371 hepatitis B virus core and envelope proteins analyzed in a cellular context. *Scientific*
372 *Reports* 9: 16178. <https://doi.org/10.1038/s41598-019-52824-z>

373 Putri, W.A., Yano, Y., Yamani, L.N., Liang, Y., Mardian, Y., Utsumi, T., Soetjipto, Lusida,
374 M.I., and Hayashi, Y. (2019). Association between quasispecies variants of hepatitis B
375 virus, as detected by high-throughput sequencing, and progression of advanced liver
376 disease in Indonesian patients. *Molecular Medicine Reports* 20: 16-24. doi:
377 10.3892/mmr.2019.10250.

378 Qin, Y., Zhang, J., Garcia, T., Ito, K., Gutelius, D., Li, J., Wands, J., and Tong, S. (2011).

379 Improved method for rapid and efficient determination of genome replication and protein
380 expression of clinical hepatitis B virus isolates. *Journal of Clinical Microbiology* 49(4):
381 1226-1233.

382 Schuppan, D., and Afdhal, N.H. (2008). Liver Cirrhosis. *Lancet*. 371 (9615): 838-851. doi:
383 10.1016/S0140-6736(08)60383-9

384 Thafar, M.A., Alshahrani, M., Albaradei, S., Gojobori, T., Essack, M., Gao, X. (2022).
385 Affinity2Vec: drug-target binding affinity prediction through representation learning,
386 graph mining, and machine learning. *Sci Rep*, 12(1):4751. doi: 10.1038/s41598-022-
387 08787-9

388 Thedja, M.D., Muljono, D.H., Nurainy, N., Sukowati, C.H.C., Verhoef, J., Marzuki, S. (2011).
389 Ethnogeographical structure of hepatitis B virus genotype distribution in Indonesia and
390 discovery of a new subgenotype, B9. *Arch Virol* 156: 855-868. doi: 10.1007/s00705-011-
391 0926-y

392 The Polaris Observatory Collaborators. (2018). Global prevalence, treatment, and prevention
393 of hepatitis B virus infection in 2016: a modelling study. *Lancet Gastroenterol Hepatol*,
394 3 (6): 383-403. [http://dx.doi.org/10.1016/s2468-1253\(18\)30056-6](http://dx.doi.org/10.1016/s2468-1253(18)30056-6)

395 Tzeng, H.T., Tsai, H.F., Chyuan, I.T., Liao, H.J., Chen, C.J., Chen, P.J., Hsu, P.N. (2014).
396 Tumor Necrosis Factor-Alpha Induced by hepatitis b virus core mediating the immune
397 response for hepatitis B viral clearance in mice model. *PLoS ONE*, 9(7): e103008.
398 <https://doi.org/10.1371/journal.pone.0103008>

399 Uzzaman, M., Chowdhury, K., Hossen, M.B. (2019). Thermochemical, molecular docking and
400 ADMET studies of aspirin metabolites. *Frontiers Drug Chemistry Clinical and*
401 *Research*, 2: 1-5. van Hemert, F.J., Zaaier, H.L., Berkhout, B., Lukashov, V.V. (2007).
402 Mosaic amino acid conservation in 3D-structures of surface protein and polymerase of
403 hepatitis B virus. *Virology*, 370: 362-372. doi: 10.1016/j.virol.2007.08.036

404 Wakefield, A.E., Yueh, C., Beglov, D., Castilho, M.S., Kozakov, D., Keseru, G.M., Whitty,
405 A., Vajda, S. (2020). Benchmark sets for binding hot spot identification in fragment-based
406 ligand discovery. *J Chem Inf Model*, 60(12):6612-6623. doi: 10.1021/acs.jcim.0c00877

407 Waterhouse, A., Bertoni, M., Bienert, S., Studer, G., Tauriello, G., Gumienny, R., Heer, F.T.,
408 de Beer, T.A.P., Rempfer, C., Bordoli, L., Lepore, R., Schwede, T. (2018). SWISS-
409 MODEL: homology modelling of protein structures and complexes. *Nucleic Acids Res.*,
410 2:46(W1):W296-W303. doi: 10.1093/nar/gky427

411 Yamani, L.N., Yano, Y., Utsumi, T., Juniastuti, Wandono, H., Widjanarko, D., Triantanoe, A.,
412 Wasityastuti, W., Liang, Y., Okada, R., Tanahashi, R., Murakami, Y., Azuma, T.,

413 Soetjipto, Lusida, M.I., Hayashi, Y. (2015). Ultradeep sequencing for detection of
414 quasispecies variants in the major hydrophilic region of hepatitis B virus in Indonesian
415 patients. *Journal of Clinical Microbiology*, 53 (10): 3165-3175. doi: 10.1128/JCM.00602-
416 15

417 Yano, Y., Utsumi, T., Lusida, M.I., Hayashi, Y. (2015). Hepatitis B virus infection in
418 Indonesia. *World Journal of Gastroenterology*, 21 (38): 10714-10720. doi:
419 10.3748/wjg.v21.i38.10714.

420

Accepted Manuscript